Rotating tomography Paris-Edinburgh cell

High Pressure Research

An International Journal

ISSN: 0895-7959 (Print) 1477-2299 (Online) Journal homepage: http://www.tandfonline.com/loi/ghpr20

Rotating tomography Paris–Edinburgh cell: a novel portable press for micro-tomographic 4-D imaging at extreme pressure/temperature/stress conditions

J. Philippe, Y. Le Godec, M. Mezouar, M. Berg, G. Bromiley, F. Bergame, J. P. Perrillat, M. Alvarez-Murga, M. Morand, Robert Atwood, A. King & S. Régnier

To cite this article: J. Philippe, Y. Le Godec, M. Mezouar, M. Berg, G. Bromiley, F. Bergame, J. P. Perrillat, M. Alvarez-Murga, M. Morand, Robert Atwood, A. King & S. Régnier (2016): Rotating tomography Paris–Edinburgh cell: a novel portable press for micro-tomographic 4-D imaging at extreme pressure/temperature/stress conditions, High Pressure Research, DOI: 10.1080/08957959.2016.1221951

To link to this article: http://dx.doi.org/10.1080/08957959.2016.1221951

Published online: 06 Sep 2016.

HIGH PRESSURE RESEARCH, 2016
http://dx.doi.org/10.1080/08957959.2016.1221951

Taylor & Francis
Taylor & Francis Group

Rotating tomography Paris–Edinburgh cell: a novel portable press for micro-tomographic 4-D imaging at extreme pressure/temperature/stress conditions

J. Philippe[a], Y. Le Godec[a], M. Mezouar[b], M. Berg[c], G. Bromiley[c], F. Bergame[a], J. P. Perrillat[d], M. Alvarez-Murga[b], M. Morand[a], Robert Atwood[e], A. King[f] and S. Régnier[g]

[a]IMPMC-CNRS, UMR 7590, UPMC Sorbonne Universités, Paris, France; [b]European Synchrotron Radiation Facility, Grenoble, France; [c]School of GeoSciences and CSEC, University of Edinburgh, Edinburgh, UK; [d]Laboratoire de Géologie de Lyon, Université Claude Bernard Lyon1, Lyon, France; [e]Harwell Science and Innovation Campus, Diamond Light Source, Chilton, UK; [f]Synchrotron Soleil, L'Orme des Merisiers, Gif-sur-Yvette, France; [g]ISIR, UPMC Sorbonne Universités, Paris, France

ABSTRACT

This paper presents details of instrumental development to extend synchrotron X-ray microtomography techniques to *in situ* studies under static compression (high pressure), shear stress or the both conditions at simultaneous high temperatures. To achieve this, a new rotating tomography Paris–Edinburgh cell has been developed. This ultra-compact portable device easily and successfully adapted to various multi-modal synchrotron experimental set-up at ESRF, SOLEIL and DIAMOND is explained in detail. An in-depth description of proof of concept first experiments performed on a high resolution imaging beamline is then given, which illustrate the efficiency of the set-up and the data quality that can be obtained.

ARTICLE HISTORY
Received 24 March 2016
Accepted 21 July 2016

KEYWORDS
High pressure; high temperature; tomography; stress; synchrotron

Introduction

The 'Paris–Edinburgh' (PE) cell in its standard design is a compact large-volume press ($\sim 25\ cm^3 \times 25\ cm^3 \times 25\ cm^3$) with a 250 t capacity and a mass of only 50 kg. Originally developed for time-of-flight neutron scattering experiments at the ISIS spallation neutron source in the U.K.,[1,2] this press has been adapted and modified for a wide range of *in situ* high pressure (HP), high temperature (HT) measurements such as neutron and X-ray diffraction, extended X-ray absorption fine structure, Compton scattering, inelastic neutron and X-ray scattering, ultrasonic studies. ([3] and references therein). In its standard configuration, by using a geometry of two opposed toroidal anvils and null-scattering metallic gaskets for neutron scattering experiments, it is possible to routinely achieve pressures in excess of 25 GPa with this press (at room temperature [4] and recently at low temperature down to 1.8 K [5]) for neutron scattering experiments. For synchrotron use, this device,

CONTACT Y. Le Godec yann.legodec@impmc.upmc.fr IMPMC-CNRS, UMR 7590, UPMC Sorbonne Universités, 4 place Jussieu, 75005 Paris, France; J. Philippe julien.philippe@impmc.upmc.fr IMPMC-CNRS, UMR 7590, UPMC Sorbonne Universités, 4 place Jussieu, 75005 Paris, France

equipped with appropriate T-cup anvils, can generate static pressures up to 25 GPa and simultaneously temperatures up to 2500 K on several mm^3 sample volumes.[6] In the simple conical anvil configuration, this press operates routinely to 15 GPa and 1500 K with sintered diamond anvils and 10 GPa and 2500 K with tungsten carbide anvils. This set-up is complementary to methods using diamond anvil cells (DAC). The larger sample volume provides excellent powder statistics and reduces problems such as poor stoichiometry, chemical separation or thermal-pressure gradients associated with small volumes in DAC. The possibility of recovering macroscopic samples from PE cell experiments is also very advantageous for *ex situ* 'post-mortem' macroscopic characterisations. As a consequence, the PE press is widely used in many European synchrotrons (ESRF, SOLEIL, DIAMOND, DESY, etc.). However, until recently, restrictions in design have limited application of PE-type devices to synchrotron X-ray diffraction/absorption microtomographic techniques. Microtomography provides a non-destructive 3D imaging/microanalysis method selective to a wide range of properties such as morphology, density, chemical composition, chemical states, structure, and crystallographic perfection with extremely high sensitivity and spatial resolution. However, the restrictive angular aperture of PE press frames (68.8° with the 4 column, and 120° with the 2 column versions, respectively) severely limits the number of projects which can be obtained during sample (*i.e.* press) rotation, effectively preventing use of the device in what is a rapidly growing application of synchrotron radiation. In this paper we describe a new rotating module for the PE cell called rotational tomographic Paris Edinburgh cell (RoToPEc), inspired from the stress cell developed in [7] and the rotator for single-crystal neutron diffraction at HP detailed in.[8] The RoToPEc permits controlled torsional shear stresses between the opposed anvils, allowing simultaneous HP and HT measurements of samples subjected to a wide range of strain regimes and provides 360° angular access in the equatorial plane (with a very high accuracy on the angle of anvils rotation) and hence full tomography data sets for *in situ* HP, HT and/or high stress analyses. Before the RoToPEc, only GSECARS at the Advanced Photon Source at Argonne National Laboratory has demonstrated the capability of performing absorption-based tomography in large-volume samples under HP, HT and high stress using a modified Drickamer cell allowing the full rotation of the sample chamber under load.[9] This device has been successfully used to study the volumetric properties of non-crystalline materials,[10] and the deformation behaviour of multi-phase composites under shearing.[11] Nevertheless, this tomography module is installed within a hydraulic press frame on a dedicated beamlime which limits the application to other 3D imaging techniques in various beamlines/synchrotrons, and especially the development of 3D imaging of samples held under extreme conditions on dedicated, high resolution imagining beamlines.

In this paper, this new device is fully described and we report the various modifications we have made to adapt the V7 PE press in order to construct our RoToPEc. A detailed description of proof of concept first experiments performed on a high resolution imagery beamline (I12 at Diamond) is then given, which illustrate the efficiency of the set-up and the data quality that can be obtained.

The new rotopec RoToPEc device

The design of a PE cell adapted for *in situ* HP/HT/high stress tomography has to satisfy several specific requirements. It should : (1) give a full angular access of 180° to the

sample by a rotating anvil system, (2) accommodate large sample volume (at least 2 mm^3) to obtain meaningful structural information on microstructure and its evolution, (3) give access to a wide pressure and temperature range (up to 10 GPa and 2500 K) and/or large deformation rates (at least $\gamma > 3$), (4) maintain the transparency of sample environment (limiting X-ray absorption, especially in the imaging mode), (5) Eliminate scattering from the gasket (in diffraction mode), so that the press is compatible with a Sollers slits system, (6) Maintain the sample geometry during compression (limit gasket lateral extrusion, which would be a source of reconstruction artefacts), (7) provide parallel, synchronised, fast (in less than 10 min for a 360° rotation) and precise (with a precision better than 0.02°) rotation under load. The rotation axis should also be perfectly perpendicular to the beam, (8) to permit the anvils to rotate independently, for example in opposite directions (for deformation) and (9) be easy to handle, portative. The press has first to fit on the ID27 Beamline at ESRF, which is optimised for performing PE cell experiments, but should be easily exportable to beamline at other synchrotrons (SOLEIL, DIAMOND, etc.), especially those with high resolution imagining capability.

Following these requirements, we designed and patented [12] a new HP device using the V7 PE press. The V7 (dimensions : 24 cm × 24cm × 41 cm) has a capacity of 450 t, that is, almost twice that of standard PE presses, but still a weight of less than 100 kg. To accommodate our new device on the PE loading frame, two significant modifications, as shown in Figure 1, have been made on the standard V7 PE press: first, the four tie rods have been elongated from 413 to 838 mm length; this provides the additional space required to accommodate rotation components (Figure 1(a)). Similar elongation of the PE press columns have been performed previously on the V7 (50%) [7] and V4 (88%) models.[13] Secondly, the piston has been modified to prevent its possible coupled rotation during anvil rotation under load (Figure 1(b)).

In our new system, both anvils can rotate independently under load, with no limitation in angle, through two sets of gear reducers and thrust bearings. A schematic 3D view with cross section of the module is shown in Figure 2. The press including the module has a total weight of 197 kg but the press can be easily disassembled in a few minutes to

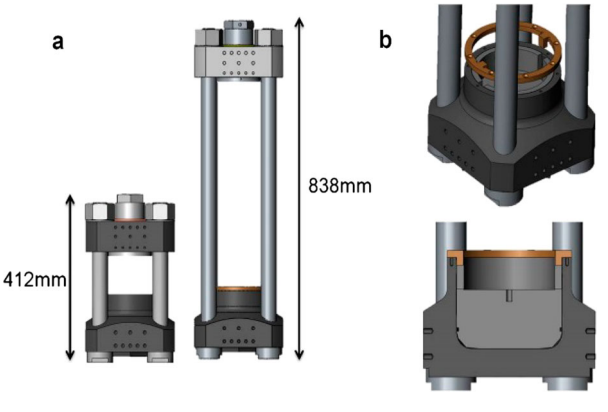

Figure 1. Two significant modifications on the V7-450 t PE press frame include (a) 103% elongation of the 4 columns and (b) modification of the piston to prevent its rotation. This is necessary as the frictional force at the roller thrust bearings is high and may cause the piston to rotate under torque or shear the O-ring seal.

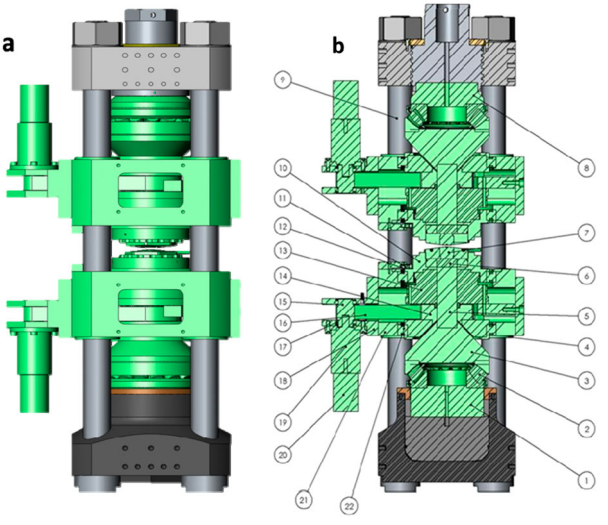

Figure 2. (a) 3-D scheme and (b) cross-section of the RoToPEc module installed on a 450 t V7-PE press: (1) modified ram and spherical roller thrust bearings, (2) spherical roller thrust bearings (29414E,SKF), (3) conical spacer, (4) guiding piece and nylon insulator on each column, (5) central piston, (6) anvils seats with WC core, (7) hexagonal-shaped anvils with WC core, (8) modified breech and spherical roller thrust bearings, (9) press columns, (10) anvils housing, (11) scanning head, (12) grating-disk (13) 160:1 Harmonic Drive© reduction gearing, (14) pulley 60 teeth (RPP5, HPC), (15) pulley 20 teeth (RPP5, HPC), (16) cog belt (RPP5, HPC), (17) ball bearings, (18) motor support, (19) 100:1 Faulhaber gear reducer, (20) Faulhaber motor (44H24BSK11R52S1), (21) sliding support and (22) ball bearings.

facilitate transport and reassembly at beamlines (Cf. Figure 3), where its integration only requires *x*–*y*–*z* translations and a rotation stage for micro-positioning of the sample along the beam.

To illustrate the working principle of the RoToPEc module, some magnified schematic cross-sections of the apparatus are presented in Figures 4 and 5. As the module is symmetrical with respect to the anvils, the explanations given below are based only on the bottom section of the module.

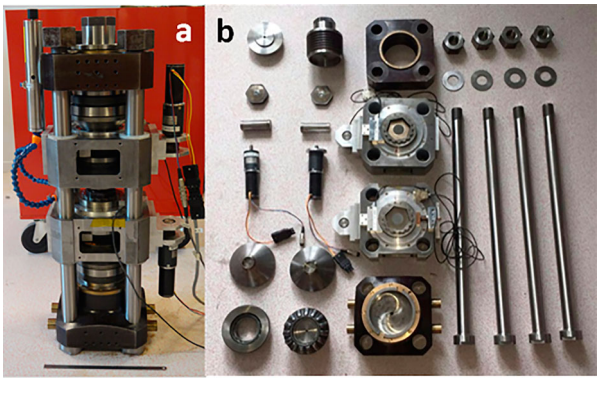

Figure 3. Assembled (a) and disassembled (b) RoToPEc device. The press including the module has a total weight of 197 Kg but the press can be easily dismounted in a few minutes for an easier transport.

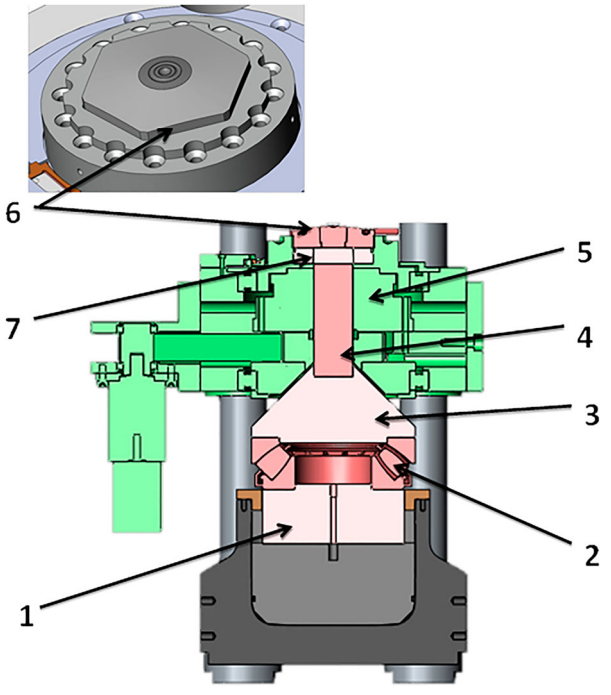

Figure 4. Magnification of the bottom part's RoToPEc module, detailing the transmission of force and therefore the generation of HP in the module. The numbers are explained in the text.

Pressure generation

As shown in Figure 4, the hydraulic ram pushes a part (no. 1); the latter transfers the force from the piston to the spherical thrust roller bearings (no. 2), which can support a maximum load of 1250 kN; the conical part (no. 3) transfers all this force on part (no. 4) mounted freely through the gearbox (no. 5), which in turns applies it on the tungsten carbide cross-section (no. 6) of the hexagonal anvil seats (no. 7). The oil pressure in the ram is generated by a computer-controlled hydraulic ('syringe') pump with a capacity of 3000 bars, while temperature is adjusted by controlling via a regulation the electrical power delivered to the furnace. This ensures a stability of pressure–temperature conditions over the computed tomography scan collection that can last several hours.

Anvils rotation under pressure

As shown in Figure 5, the anvils (A) are inserted in the housing (C), which is fixed to the output of the reduction gearing (D). This gearbox (D) can produce a maximum local torque of 892 Nm, the latter being the main limiting factor of the RoToPEc. The gearbox (reference: SHG-32-160-2UH from HARMONIC DRIVE) has a reduction ratio of 160:1 and a yield of 0.6 at low speed; therefore 9.3 Nm must be applied to the input of the gearbox to generate the necessary torque for rotation of the anvils. For this, a gear with tailored dimensions (E) is fixed to the input of the gearbox and associated to a timing belt (F) and a second gear (G). This belt-pulley system has a further reduction ratio of 3:1 and a yield of 0.8. Therefore, the pulley attached to the motor shaft must provide

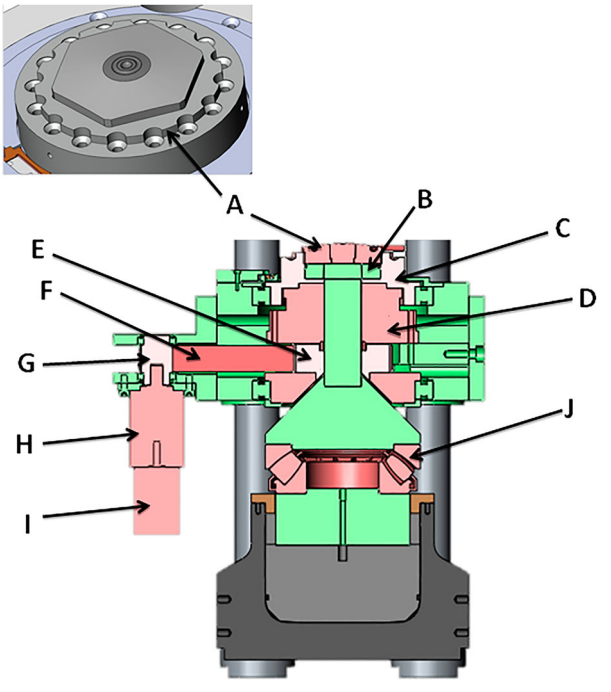

Figure 5. Magnification of the bottom part's RoToPEc module, detailing the anvils rotation system. The labels are explained in the text.

3875 Nm to rotate the anvil. However, the gear motor consisting of a motor (I) allowing 197.8 mNm of torque and a reducer (H) of ratio 100 with a yield of 0.65 can provide an oversized torque of 12,857 Nm, which is more than enough to generate rotation of the anvils subjected to maximum stress. The rotation of the pulley is driven by ball bearings (no. 17 in Figure 2) using an original motor support (no. 18 in Figure 2) which is fixed to a sliding support (no. 21 in Figure 2). The latter, through tubular nylon parts, slides with precision in compression along the columns of the press. On this sliding support, the ball bearings (no. 22 in Figure 2) offer a very high precision guide for the rotation of the anvils.

Accurate control of the anvils' rotation

The precise angular position of one anvil can be determined from the output of the encoders on the motors, assuming that the system is perfect, and lossless, with the various reduction ratios (in principle, 48,000 motor rotations should give one anvil rotation). Although this method is used in other HP rotating systems [7–9,14] (as shown below), we found that it was not sufficient for high-quality tomographic reconstructions, and another solution had to be found. In the RoToPEc, we instead control the motors with two encoders placed directly on the anvils. As shown in Figure 6, an optical encoder consisting of a fixed optical reader (A in Figure 6: NUMERIK JENA scanning head RIK4-2C 142/18000 K0-WZ) and a moving optical disk (B in Figure 6: NUMERIK JENA aluminium grating-disk RS142/120/18000) anchored to the anvil provide feedback on anvil positioning. The motor interfacing system consists of housing for power electronics containing two

interfaces (Faulhaber MCBL-3006S) dedicated to power supply and control the rotation speed of each of the two anvil motors. This system also provides highly accurate servo rotation to each anvil. The angular resolution of the rotation system is 0.005°. At full power, the driving mechanism allows complete rotation of the anvils (*i.e.* 360°) under maximum stress in about 9 min. Figure 7 shows the error obtained by comparing the value obtained by the motors encoders with those exact, given by the anvils encoders during a full anvil rotation at low pressure (7 t): an error of the motor's encoders up to 2.25° was observed. This figure clearly demonstrates the need for a direct measurement of the anvil rotation with an encoder positioned thereon.

Electronics and software control

An electronic box has been built following the automation structure detailed in Figure 8. It allows monitoring and control of two motors (FAULHABER 4490 series) rotating both the anvils. It also ensures the reading of the two incremental encoders (Numerik Jena) coupled to the anvil, the encoders motors and port enabling communication between the control software and the electronic box. The PC-interface communication is provided by an RS232 serial link or a Transmission Control Protocol/Internet Protocol Ethernet link and can be installed easily on any computer or laptop. Our home-made user-friendly application on Labview software can operate individually or simultaneously on both motors and send instructions for rotation to specified angles or speed. It also displays continuously the real position of each anvil offering off-line control for the RoToPEc module. With our control device, complicated profiles can be followed by the anvils. For example, the RoToPEc has been recently extended to forced-oscillation method at HP and HT. These torsional forced-oscillation experiments provide measurements of shear modulus G and the associated strain energy dissipation Q_G^{-1}. For that, the sample and an elastic standard of know modulus and negligible dissipation, connected mechanically in series, are subjected

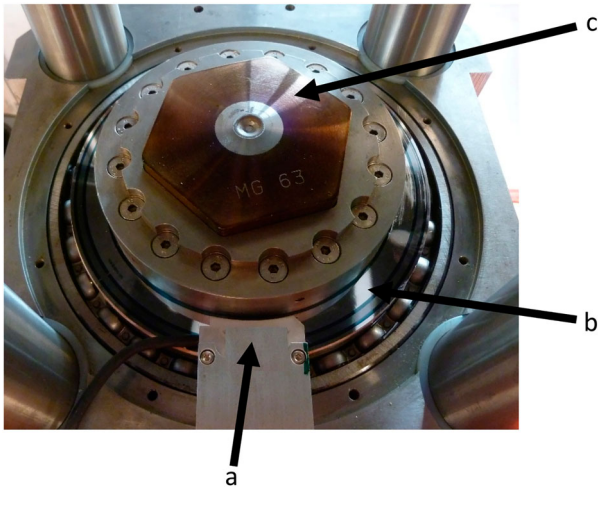

Figure 6. An optical encoder (B) attached to the housing of the anvil (C) is used to measure the angular position of the anvils with a resolution of 0.005°. A scanning head (A) allows reading the optical encoder.

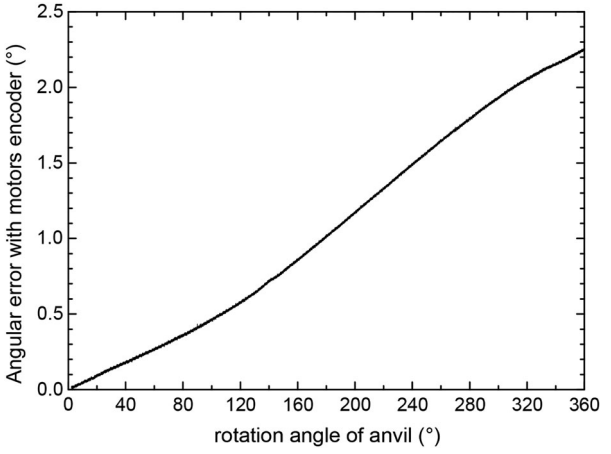

Figure 7. Angular error obtained by comparing the value given by the motors encoders with those exact, given by the anvils encoders during a full anvil rotation at low pressure (7 t).

to a low-frequency sinusoidally time varying torque. Our software allows to configure this desired profile (sine), its amplitude, period, number of cycle and synchronisation step. After defined synchronization step, a 2D array is generated and downloaded to the memory of our controllers. Motors, and therefore the anvils then follow perfectly the complicated profile set by the operator. Also, at any defined synchronization step, a transistor-transistor logic signal can be sent to an external instrument, for example, an X-ray camera to perform an imagery acquisition.

Heating configuration

The heating system for the RoToPEc module is different from the standard PE press, as illustrated in Figure 9(a). The electrical feed-through is provided by an external copper

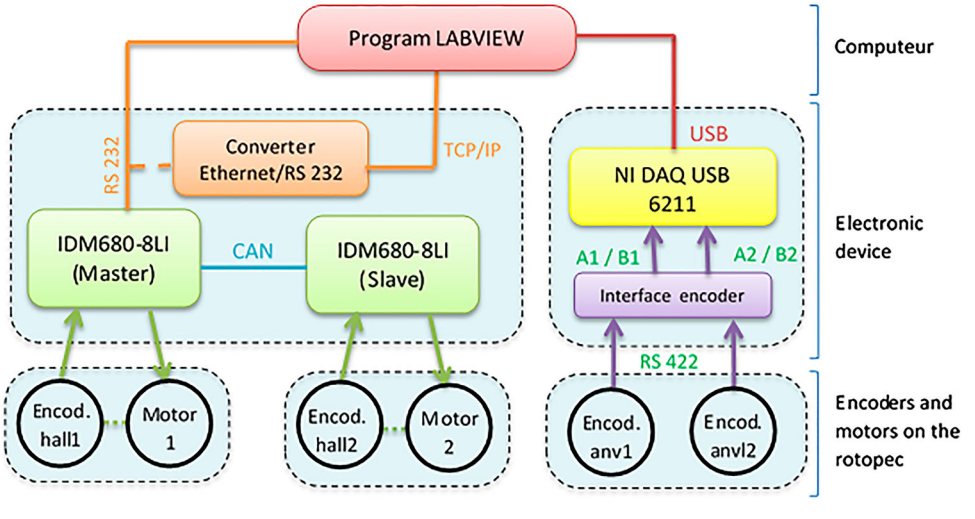

Figure 8. Automation structure of RoToPEc module.

piece which is compressed against the anvils housing using a spring. The specific shape of this copper piece allows the housing to rotate without interference during anvils rotation. Also, because the HT experiments can cause multiple damage to our system (anvils, encoders, bearings, etc.), it is necessary to cool the anvils and the press during the HT runs. For that, a Coldstream Air Gun (from Meech) is used to rapidly cool (with a cold airflow) the various components. Its size and simple magnetic base permit easy installation on the RoToPEc (Figure 9(b)). The cold air produced by the Vortex Tube is easily directed on to the anvils to be cooled via a knuckle trunking. The hot air created by the opposite end of the Vortex Tube flows simply into the atmosphere. The cold airflow is as low as 50°C below the inlet air temperature, making this cooling device extremely efficient. With this cooling system, we observed (by means of a thermocouple placed on the anvil) that the temperature of the anvils does not exceed 60°C when the sample is at about 2000°C. Without this system, the temperature of anvils and press reaches rapidly about 120°C, damaging many crucial pieces, including the Teflon around columns (which is useful for electrical insulation of the lower part of the RoToPEc) and the optical disk (which is used for measuring the rotation angle); as such this cooling system is essential for the RoToPEc. Also, to prevent excessive temperature rise of the optical discs, thick pyrophyllite rings are inserted between the metal parts of the press and optical discs for their thermal insulation and protection (Figure 10(a)). An external aluminium casing is finally added to protect the disks from oil, dust, scratches and in general to avoid the disks being touched or damaged during the installation of the RoToPEc (Figure 10(b)).

Pressure and temperature operating domains

All standard anvils of the PE press can be used in our RoToPEc system. Hence, in the simple conical anvils' configuration, the RoToPEc operates routinely to 15 GPa and 1500 K with sintered diamond anvils and 10 GPa and 2500 K with tungsten carbide anvils. This domain has been recently extended by using the toroidal profile developed in [15] and we reached 13.6 GPa and 2400 K with tungsten carbide anvils. The usual sample assembly is essentially the same as for the original PE press, using a boron epoxy transmitting medium. A Poly-ether-ether-ketone (PEEK) or Lexan ring is added around the gasket to

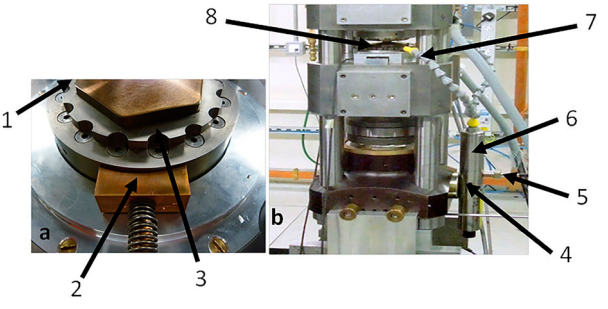

Figure 9. (a) Heating system of the RoToPEc with the power input elements : (1) housing for anvils; (2) copper slider ; (3) compression spring; (b) Cooling system showing in operation the Coldstream Air Guns: (4) hole for hot air ventilation; (5) compressed air; (6) Coldstream Air Guns; (7) Flexible Knuckle Trunking; (8) anvils.

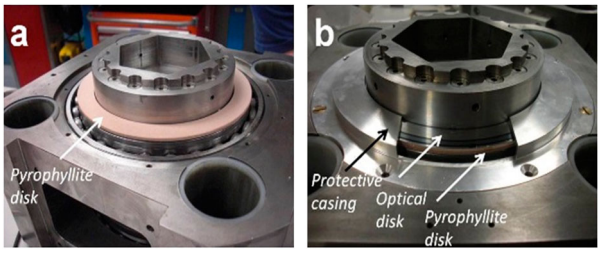

Figure 10. (a) Internal 2.1 mm pyrophyllite ring (from Elit Stumatite) and (b) external aluminium covers are used for protection of the optical disks.

limit the lateral extrusion of the set-up during compression, as it can be source of motion artefacts in the tomographic reconstruction. This containment ring also helps one to hold a large X-ray window between the anvils suitable for full-field imaging mode in micro computed tomography, and also provides a homogenous background for white field corrections.

Synchrotron imaging experiments

Independent and controlled rotation of each anvil enables operation in shearing (one anvil rotates while the other is stationary) or deformation modes (both anvils rotate in opposite directions) under HP and HT conditions. Hence, our portable device can operate in various modes (Cf. Figure 11). The ability to fully rotate the sample chamber under extreme conditions overcomes the usual limited angular aperture of ordinary HP set-ups, allowing complete sets of tomographic projections to be acquired, in both full-field imaging (where a large (approx. 2 $mm^2 \times 2$ mm^2) monochromatic (or pink) X-ray beam is used to collect 2-D radiographs) or micro-diffraction modes since our RoToPEc is fully compatible with the Sollers slits system of ID27 at ESRF (scanning with a pencil beam of FWHM 3 $\mu m^2 \times 3$ μm^2 at several projection angles). Additionally, on ID27 of ESRF, it is now possible to switch during an experiment between the two microtomographies (absorption and

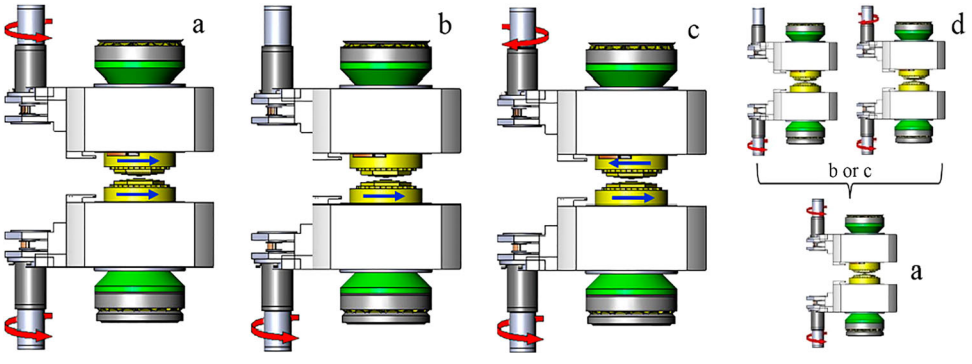

Figure 11. The various operation modes of the RoToPEc: (a) HP and HT X-ray microtomography, (b) and (c) HP and HT stress X-ray diffraction (or ex situ synthesis); (c) mode permits a higher rate (and speed) of deformation (d) or a combination of type (b then a) or (c then a) for HP, HT and high stress X-ray microtomography.

diffraction) by keeping the same sample under HP, HT and stress conditions. It is done automatically (without going into the X-ray hutch) via automatic movements (Cf. Figure 12) and in less than a minute.

Hence, our portable device has been easily and successfully adapted to various multi-modal synchrotron experimental set-up at beamlines ID27 (ESRF), PSICHE (SOLEIL) and I12 (DIAMOND).

The potential of our new equipment for *in situ* synchrotron experiments has been clearly illustrated by preliminary results recently obtained from these facilities on many scientific cases: direct visualisation and quantification of melt migration at extreme pressure–temperature–stress conditions,[16] X-ray diffraction computed tomography of C_{60} sample,[17] determination of the density of amorphous materials at extreme conditions,[18] anelasticity and attenuation in olivine at upper mantle conditions and seismic frequencies,[19] etc.

Example: in situ *microtomographic imaging at simultaneous HP–HT–high stress*

To demonstrate the potential for the RoToPEc system to provide high resolution *in situ* imagining, we performed a series of experiments on the Joint Engineering, Environmental and Processing i12 general imaging beamline at the DIAMOND synchrotron facility in Oxfordshire, U.K. This beamline utilises X-rays created by an insertion device, with an energy range of 50–150 kEV, tunable with a monochromator. The small size and weight of the RoToPEc meant that it could be installed on the inner hutch of this beamline (as described in [20]), giving a higher X-ray flux. The RoToPEc was installed within less than

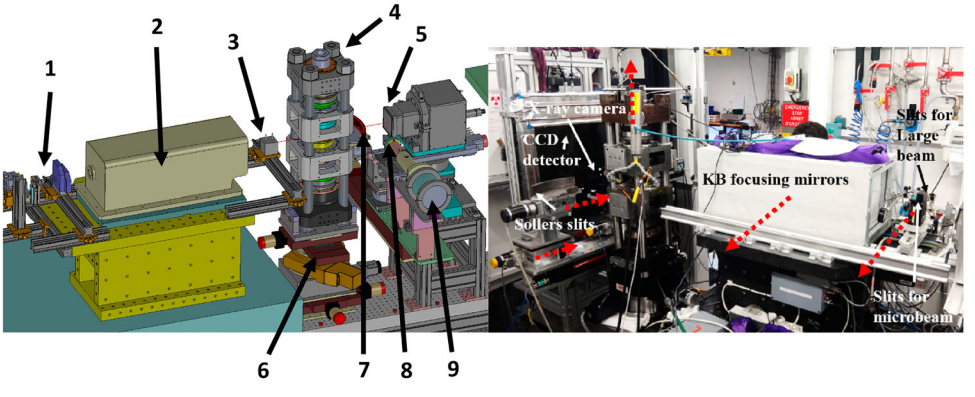

Figure 12. Scheme and photograph of the set-up for absorption and diffraction microtomography experiments at beamline ID27 of ESRF. (1) X-rays slits; (2) KB focusing mirrors; (3) ionisation chamber; (4) RoToPEc ; (5) Frelon or CCD detector; (6) Positioning motors for the press; (7) Sollers slits; (8) Scientillator and microscope objective; (9) Absorption CCD camera. The RoToPEc is installed in various high-precision positioning motors. In absorption microtomography, the transmitted X-rays are converted into visible light using a single-crystal YAG scintillator. A mirror reflects the visible light into a high resolution CCD CoolSNAP HQ2 Photometrics detector placed on translation motors (y, z). When diffraction microtomography is settled, this detector moved and is replaced by a Sollers slits system. Also, the KB focusing mirrors are positioned to define a focused X-rays beam of $3\ mm^2 \times 3\ mm^2$. The various automatic movements to move from absorption microtomography mode to diffraction microtomography mode are symbolised by the red dotted arrows.

2 h in the inner hutch of the i12 beamline on an aluminium alloy stage on one of the standard beamline optics stages to allow exact sample centring. This stage also allowed slight tilts in the *X* and *Y* directions in the axis rotation of the sample to be adjusted, to minimise noise and artefacts in reconstructions. The rotational axis of the press was aligned with the X-ray beam and camera (PCO 4000) using a small (0.5 mm) Pt sphere placed within the centre of a dummy assembly within the press frame. The PCO camera (beamline module 4) is a CCD detector with a 4008×2672 array of $6.5\ \mu m \times 6.5\ \mu m$ pixels, with $3.3\ mm \times 2.8\ mm$ field of view, giving a pixel scale of approximately 1.3 μm. Pressure and temperature were monitored and controlled during experiments using control systems within the experimental hutch. The press drive system was controlled remotely from outside the hutch.

Due to limitations in machine time available, RoToPEc motor rotation and beamline camera shutter software were controlled separately rather than being fully integrated into the same control system. However, subsequent experiments performed at ID27, ESRF have demonstrated that RoToPEc control software is easily integrated with beamline software to facilitate data collection. In order to obtain tomographic scans at DIAMOND, RoToPEc anvils were continuously rotated through an angle of 180° at a constant speed, and the X-ray camera programmed to take projections at the correct time interval to ensure that 1501 projections were taken for every scan. The benefit of this approach was that anvils could readily be left to rotate during sample annealing, and data later binned to provide a time-resolved series of scans of the sample. Exposure times of 1.73 s proved to be adequate to ensure good data quality for the sample investigated; movement of the motors over this exposure time produced no noticeable effect on projection quality. Before and after each scan, 40 flat field and 40 dark current images were taken to normalise projections. Flat field images were obtained through air by driving the sample stage so that no parts of the assembly or press frame were in the field of view of the camera. Dark field images were obtained by then closing the experimental shutter. Relative intensities in processed images were then self-corrected using beamline software. The majority of tomographic scans were collected using a monochromatic beam energy of 53 kV.

Samples were chosen for initial tomography scans to test the capability of the RoToPEc for microtomographic imaging under HP, HT, high stress conditions. Synthetic, polycrystalline forsterite (Mg_2SiO_4) capsules (Figure 13) were prepared by hot-pressing cylinders of powdered forsterite (pre-synthesised in a piston-cylinder press) for several days at 1200°C in air. Cylinders were then shaped and drilled to produce 3 mm outer diameter, 1 mm inner diameter capsules with lids. Capsules were loaded with a mixture of natural olivine (Fo_{92} composition) and finely powdered Fe–S, with the approximate volume proportion 20% Fe–S. Considerable X-ray absorption contrast between the Fe–S and olivine/forsterite should be readily apparent, as this, coupled with a simply initial sample geometry, was used as a test of typical voxol resolution achievable under different conditions.

After some experimentation, we adopted a sample-detector distance of 300 mm to ensure a high attenuation contrast. Longer distances enhanced the phase contrast effect, but any advantage was offset by a greater reduction in contrast between the phases of interest and reduced transparency of the boron–epoxy gasket. Due to limitations in beam size in synchrotron tomography experiments, gasket transparency is of key interest because during rotation, the gasket is never fully within the X-ray beam,

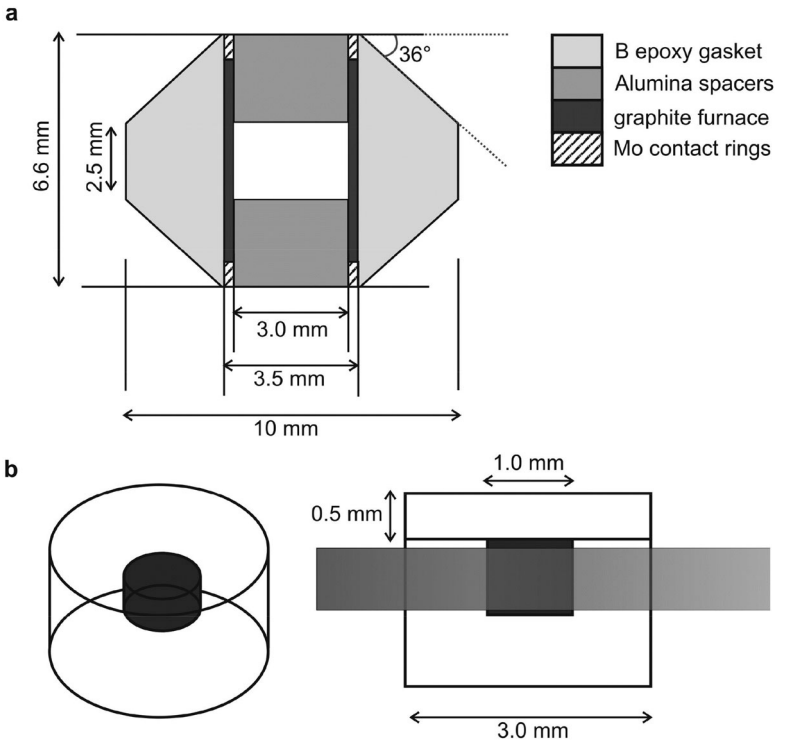

Figure 13. Gasket and capsule design used in RoToPEc experiments at DIAMOND i12 (The PEEK ring around the gasket is not shown in this figure). (a) Design of gasket, with sample located in central region (unshaded) within amorphous boron–epoxy gasket containing internal graphite resistance furnace. Machinable alumina spacers are used to position the sample. (b) 3-D and schematic view of the polycrystalline synthetic forsterite capsule (white) with central region (dark grey) filled with powdered Fe–S and natural olivine. Transparent grey box highlights the approximate volume of the capsule imaged *in situ* during HP–HT–high stress experiments.

and loss of transparency therefore results in artefacts during data reconstructions. All scans were reconstructed using DIAMOND in-house software using a standard, filtered back-projection algorithm. Final scans were produced with a calculated voxol resolution of approximately 2 µm, which is comparable to the resolution routinely available with commercial, large-volume lab-based microtomographic devices.

Tomographic scans were taken of a series of samples at (1) room temperature and pressure, (2) room temperature and HP during various stages of annealing (to provide time-resolved snapshots of textural equilibrium), (3) HT and HP, and (4) simultaneous HT, HP during ongoing deformation, to provide an assessment of resolution and data quality under different conditions. A final tomographic scan was also taken of all quenched samples *in situ*. Samples were removed and later scanned (within full gasket assemblies) using an in-house built computed tomography system at the University of Edinburgh, both to compare data quality and allow full examination of volumes of the sample obscured during *in situ* scans by the RoToPEc anvils. Additional samples were also prepared for examination by scanning electron microscope (SEM), to ground-truth textures inferred from tomographic reconstructions.

Quality of tomographic reconstructions

Scans produced sharp, high-quality tomographic reconstructions with a voxol size of ~2 µm. Sharpness of individual scans was variable, however, as illustrated in Figure 14. All scans suffer some slight reduction in quality due to an inherent 'judder', presumably arising from the fact that the gearing/timing belt assembly used does not result in purely continuous anvil rotation. This is evident from close examination of the sinograms, where regular movement results in a symmetrical, 'frilly' edge to the stacked sonogram images. Within each sinogram, each horizontal line of pixels represents a single projection at a given angle. The wave-like edge of the sinogram therefore represents a systematic 'back and forth' translation of the whole sample volume as the motors rotate the stack. The wave is actually more pronounced in room temperature scans compared to HT

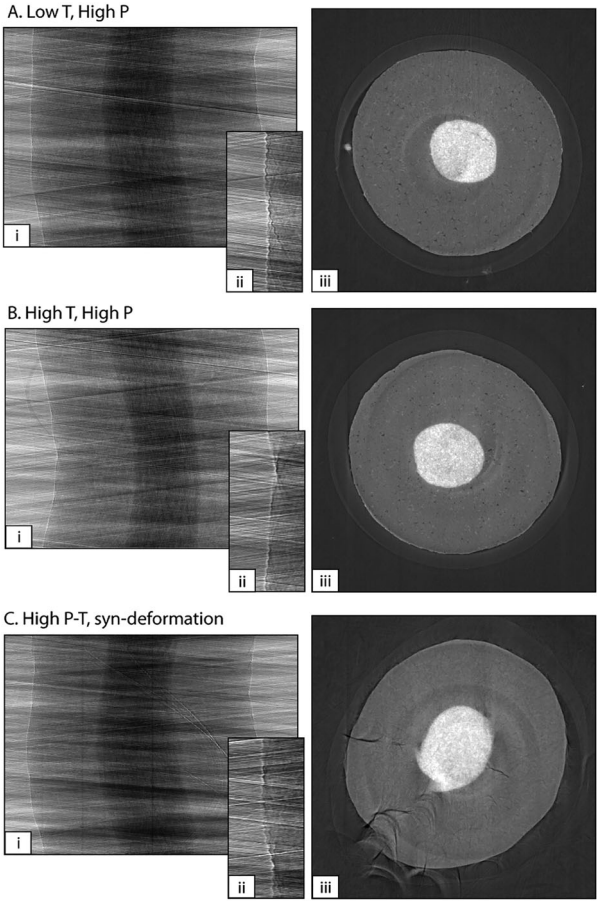

Figure 14. Examples of scan quality during DIAMOND imagining experiments for (A) scans obtained at HP but at room temperature, (B) scans obtained at HP and HT, and (C) scans obtained at simultaneous HP, HT and during torsional deformation (differential anvil rotation). In each case (i) is the intermediate sonogram image of the sample, (ii) is a magnified view of the edge of the sample volume (capsule) highlighting slight aberration due to judder in the sample rotation, and (iii) is the resulting slice from each sonogram, showing a reconstructed 2-D section through the central region of the sample, greyscaled as a function of X-ray absorption.

scans, although the reasons for this are not immediately apparent, and maybe be related to gradual warming of many of the components of the RoToPEc press frame during HT annealing. This judder is then reflected in the quality of the reconstructed sample slices. However, reduction in reconstruction quality is not prohibitive, and the systematic, regular nature of the wave means that it could be readily minimised by post-scan data processing. In the syn-deformation sinogram, the waveform is more asymmetric, and overall the lines are less sharp. This is probably due to sample movement and textural evolution during the scan, resulting in blurring in the scan reconstructions.

Figures 15 and 16 show two examples of time-resolved reconstructed slices, and stacked reconstructed 3-D images of the inner volumes of capsules from two experiments, DLS3 and DLS5, both run at an oil pressure of 120 bars and heating power of 350 W. Previous on-line and off-line experiments indicate that 120 bars corresponds to a sample pressure of approximately 3 GPa. The i12 beamline used did not, at the time, have the capability of performing diffraction analysis of samples. As such, sample pressure could not be determined using, for example, known equations of state of internal calibrants, as is routinely done in PE cell experiments. Similarly, run temperature could not be determined, except by comparison with previous experiments, and thermal evolution of the sample could not be determined, notably onset of melting of Fe–S. Again, previous experiments and the observed empirical relationship between heating power and run temperature suggest that 350W corresponds, at 3 GPa, to a sample temperature of 1600 ± 100°C. Subsequent to the work described here, i18 has been updated and *in situ* diffraction is now possible.

Time series shown in Figures 15 and 16 indicate textural evolution in the samples during annealing and then deformation. Using ImageJ [21] for post-reconstructing

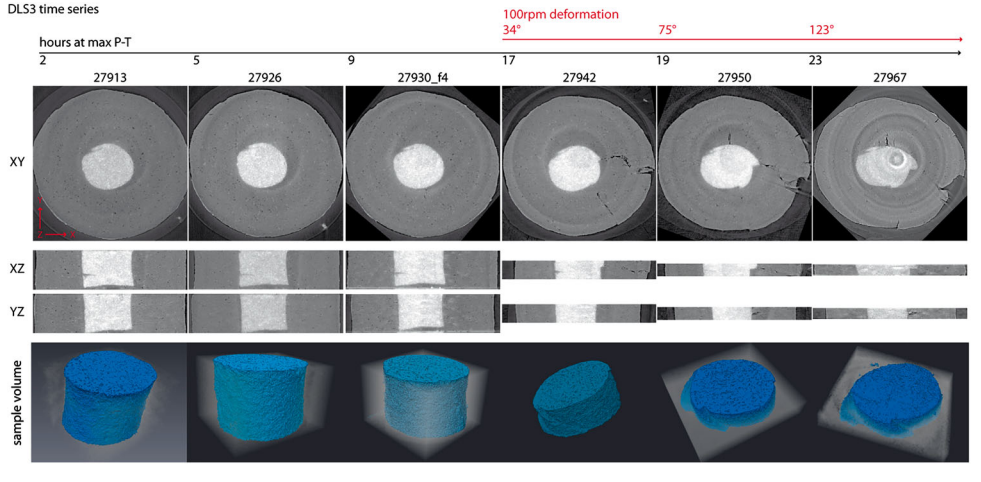

Figure 15. Textural changes in sample DLS3, shown by orthoganol slices through tomographic reconstructions, and the segmented central Fe–S-bearing region to show changes in 3-D shape. Orthoganol slices are zoomed into the central sample portion (field of view: 3 mm × 3 mm): white: Fe–S+olivine, grey:forsterite capsule, dark grey: graphite furnace surrounded by gasket. Scans obtained as a time series, left to right, during annealing at high-P, T after 2, 5 and 9 h, respectively, and then after torsional deformation corresponding to a total differential anvil rotation of 34°, 75° and 123°, as described in the main text.

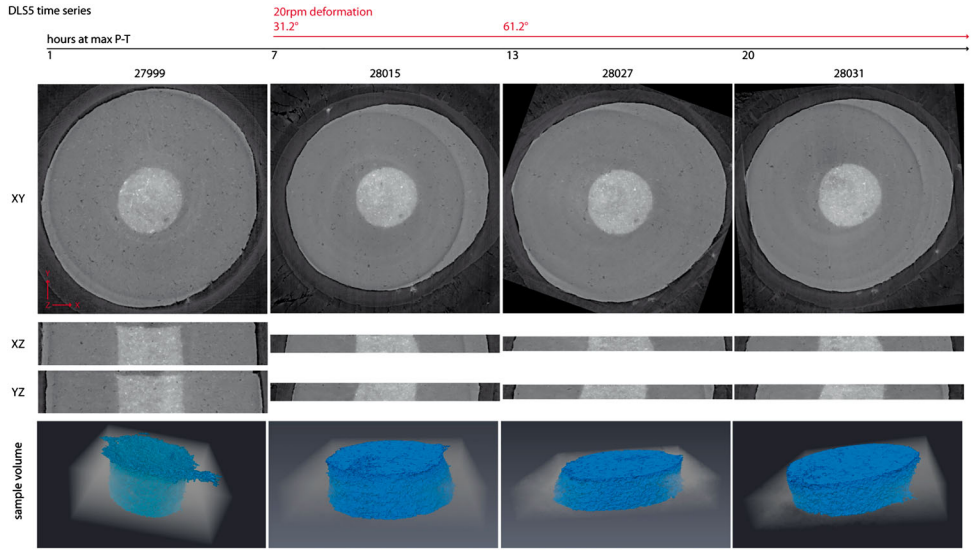

Figure 16. Textural changes in sample DLS5. Key as in Figure 15. Scans obtained after annealing for 1 h, then after slower deformation with a total differential anvil rotation of 31.2°, 61.2°, and after further annealing for 7 h, respectively.

processing, scans have been rotated to ensure the same sample orientation for each orthogonal slice, and greyscale ranges have been normalised for each scan. In addition, a fast volume reconstruction of the central Fe–S rich zone has been created using the 'magic wand' seeding tool combined with global thresholding to pick out the central bright volume, using the Avizo Fire™ segmentation tool kit. The volume fraction of Fe–S in the central portion of the capsules is significantly above the estimated percolation threshold for Fe–S melt in olivine,[22] and during the large strain-rates used during deformation, we would expect to see significant Fe–S melt mobilisation and outward migration. From the reconstructed data it is clear, however, that no significant changes in texture (and Fe–S mobilisation) have occurred. This indicates that temperatures were almost certainly too low to significantly melt Fe–S under the run conditions. However, it is apparent that changes in the sample volume with time can be readily determined, and considerable vertical compression and outward extrusion of the central sample volume occurred during progressive deformation, as might be expected for a relatively weak Fe–S sample close to its melting point (in contrast to the surrounding forsterite which has a significantly higher melting point). Comparison of the textural evolution shown in Figures 15 and 16 indicates that torsional deformation of the entire sample gasket results, ultimately, in sample shortening. The more rapid sample deformation in Figure 15 (100 rpm motor rotation, corresponding to a differential anvil rotation of 45°/h) additionally results in brittle fracture of the forsterite capsule, and extrusion of the Fe–S–olivine mixture. In comparison, slow deformation of the sample shown in Figure 16 (20 rpm motor rotation, corresponding to a differential anvil rotation of 9°/h) results only in ductile deformation of the sample assembly, and significant sample shortening. SEM imagining of recovered samples supports these textural observations. It is clear that there has not been any significant

mobilisation of Fe–S, as would be expected above the Fe–S melting point, and that Fe–S and olivine particles are still finely distributed within the central region of the samples.

As can be observed in Figures 15 and 16, reconstructed slices contain faint ring artefacts. Such artefacts typically occur in reconstructions due to slight miscalibration of the sensitivity of detector elements, although may also occur due to insufficient exposure in particularly attenuating samples. In the present study, we attempted to reduce such artefacts by taking 20+ flat field images before and after each run, to normalise any affect due to variation in beam intensity with time. We also varied beam energy and sample-detector distance during initial sample scans to minimise artefacts in sample reconstructions whilst maximising attenuation contrast within the sample volume (between olivine and Fe–S) and minimising attenuation between the sample volume and surround sample assembly (gasket and graphite furnace). Increase in the extent of artefacts during sample annealing and vertical compression/lateral extension of the central Fe–S rich region (Figure 15) suggests that high attenuation of the Fe–S rich volume of the samples is the main cause of ring artefacts. No attempt was made to post-process reconstructions and remove artefacts, as it was found that the extent of these had minimal influence on 3-D volume reconstructions. However, in future the extent of ring artefacts could be significantly reduced by increasing beam energy during progressive scans, and to adopt commonly used post-processing techniques (*e.g.* in [23]).

Figure 17 shows higher resolution CT 3-D reconstructions of the central Fe–S rich volume from experiment DLS3. Micron-scale resolution in the reconstructed dataset is sufficient to show 3-D distribution of the Fe–S phase, which can be readily imaged by segmenting data to highlight only the most attenuated portion of the sample. Optical examination of recovered sectioned samples by Scanning Electron Microscope ground truths these reconstructions. It is evident from the data that minimal aggregation of Fe–S occurs during progressive annealing and deformation, although CT data and SEM images do indicate some textural development of the Fe–S particles. Quality of reconstructed tomographic data means that more quantitative textural analysis of the samples can also be readily performed. Quant3D [24] analysis was conducted on binarised images in order to determine any development of preferential fabrics within the samples during annealing and deformation. Results of analysis on sample DLS3 (the sample shown in Figure 15) is summarised in Figure 18. The Star Distribution Length calculates the mean length of an object (*i.e.* segmented particle) in various orientations from a number of arbitrarily generated points within the dataset. Lengths from 2000 points were analysed over 513 orientations, or uniform distribution. The 3-D rose diagrams shown in Figure 18 reflect the distributions of particle lengths at these orientations. Figure 18 shows comparable data on Star Volume Distribution, which works in a similar way but models instead 3-D cones emanating from points of origin, rather than lines, therefore describing more of the texture of the binarised particles. An anisotropic fabric in these types of analysis will result in an anisotropic rose diagram, although neither type should be affected by the overall shape of the sample volume. In each analysis shown in Figure 17, the vertical axis of the diagram is the axis of rotation of the sample (*i.e.* the compression direction) and the horizontal plane is perpendicular to σ_3.

All samples show flattening of fabrics during the experiments, suggesting that particles become more elongate and aligned parallel to the plane of the torsional deformation

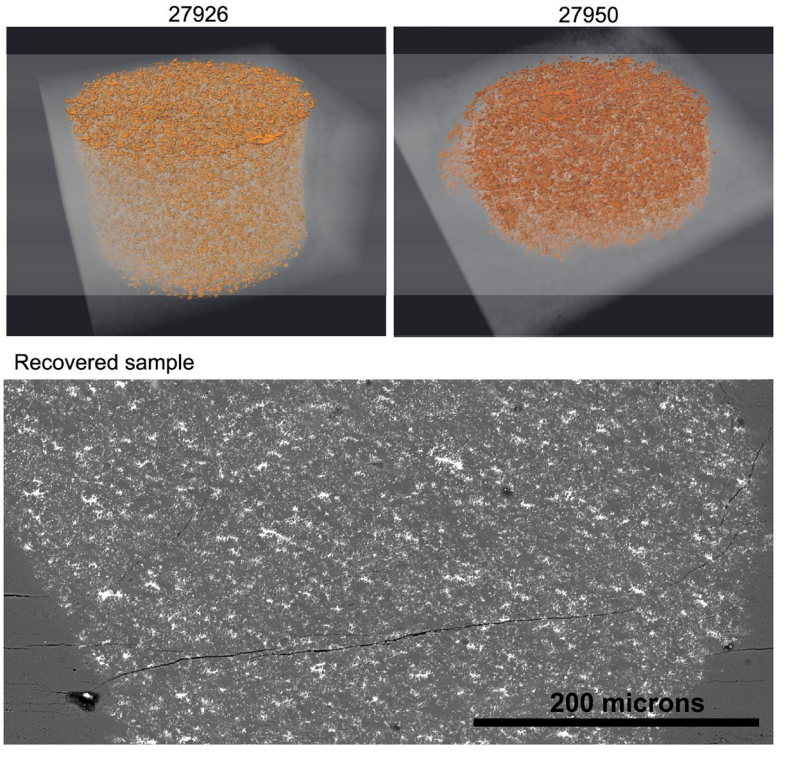

Figure 17. Top: 3-D reconstructions of the central sample volume from sample DLS3 rendered using Avizo Fire™ Data has been segmented so that only the most attenuating regions of the sample, corresponding to the Fe–S phase, are shown. The first image shows distribution of Fe–S after 5 h annealing, and the second image, distribution after 17 h annealing and after deformation (differential anvil rotation of 75°) as shown in Figure 15. Bottom: SEM back-scattered electron image of recovered sample (sectioned vertically so that the image shows a cross section through the main sample volume with anvil compression top to bottom), showing distribution of Fe–S (white) within olivine (grey) within the sample volume. Textures show dissemination of fine particles of Fe–S throughout the central sample volume, with possible development of fabric during progressive annealing/deformation, especially in larger Fe–S particles.

(*i.e.* perpendicular to the direction of compression). Some flattening occurs during compaction, and this is slightly accentuated during annealing at HP and HT, presumably due to sample recovery from initial pressurisation, concurrent with gasket flow. However, flattening clearly becomes more pronounced during deformation. There is no evidence for alignment at an angle to the shear plane, as would be expected if the Fe–S were molten.[25] Anisotropic alignment of particles is not expected as torsional deformation of the sample cylinder, although from Figure 18 it is clear that there is development of anisotropy during the later stages of the experiment. This most likely arises from the development of larger scale brittle deformation within the sample, as noted above.

To conclude, preliminary experiments indicate that the RoToPEc can be readily used to track textural development in samples at HP, HT and also simultaneous HP, HT, stress. Resolution of reconstructed data sets is comparable to tomographic studies of quenched material of comparative volume (mm^3) using commercially available equipment. Furthermore, minimal additional data processing is required, and reconstructed data can be

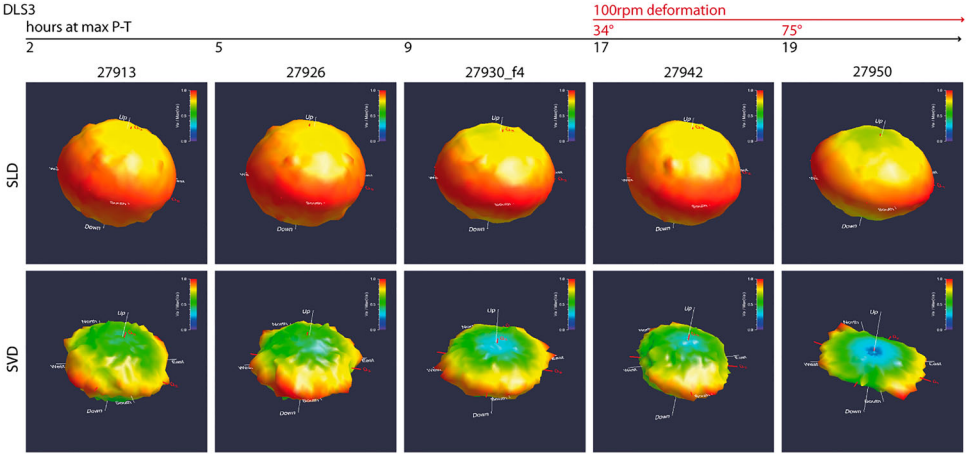

Figure 18. Example of textural analysis of reconstructed data. Fabric analysis of sample DLS3 using Quant 3D software (see main text for more details) showing results for the 5 data sets shown in Figure 15. Both fabric indicators suggest a horizontal fabric may be created by particles in the central sample volume (Fe–S+olivine) during annealing, which is then further enhanced during deformation.

interpreted and analysed using standard protocols. As such, the potential for the RoToPEc to provide time-resolved insight into textural development in samples under extreme conditions is considerable.

Conclusions

To conclude, we reported the development of a new HP rotating cell 'RoToPEc' for tomography measurements under extreme pressure, temperature and stress conditions. Based on the V7 PE press, this cell is portable and can be readily installed on most synchrotron facilities to take advantage of the diversity of 3D imaging techniques available at various beamlines. The combination of extreme conditions and X-ray microtomography provides a novel insight into the evolution of microstructure, phase distribution, strain-state and volume changes of materials under extreme P/T/stress conditions. This covers a wide range of potential studies in physics, chemistry, geology, earth, planetary and materials sciences. Although not discussed here, the 'RoToPEc' offers also new perspectives in neutron tomography.

Acknowledgements

We acknowledge the European Synchrotron Radiation Facility, the Synchrotrons DIAMOND and SOLEIL for the allocation of beamtime. We are grateful to S. Bauchau, G. Garbarino, J.P. Itié, N. Guignot, J.L. Hodeau Y. Wang and S. Redfern for valuable inputs and discussions, and to Kate Dobson for assistance with DIAMOND experiments. We thank Diamond Light Source for access to beamline i12 (EE9185).

Disclosure statement

No potential conflict of interest was reported by the authors.

Funding

This work was financially supported by the French 'Réseau Hautes Pressions', the Agence Nationale de la Recherche [ANR-2011-BS08-018], a grant 'Instrumentation aux limites 2013', the 'Institut National des Sciences de l'Univers' of CNRS, and the UK National Environmental Research Council [NE/I016333/1 and support of Ph.D. student M. Berg]. We thank Diamond Light Source for access to beamline i12 (EE9185) that contributed to the results presented here.

References

[1] Besson JM, Nelmes RJ, Hamel G, Loveday JS, Weill G, Hull S. Neutron powder diffraction above 10-Gpa. Physica B. 1992;180–181:907–910.
[2] Klotz S. Techniques in high pressure neutron scattering. CRC Press -Taylor and Francis; 2013.
[3] Le Godec Y, Hamel G, Martinez-Garcia D, Hammouda T, Solozhenko VL, Klotz S. Compact multi-anvil device for *in situ* studies at high pressures and temperatures. High Pressure Res. 2005;25:243–253.
[4] Klotz S, Besson JM, Hamel G, et al. Neutron powder diffraction at pressures beyond 25 Gpa. Appl Phys Lett. 1995;66:1735–1737.
[5] Klotz S, Strässle T, Lebert B, d'Astuto M, Hansen T. High pressure neutron diffraction to beyond 20 GPa and below 1.8 K using Paris–Edinburgh load frames. High Pressure Res. 2016;36:73–78.
[6] Le Godec Y, Hamel G, Solozhenko VL, et al. Portable multi-anvil device for in situ angle-dispersive synchrotron diffraction measurements at high pressure and temperature. J Synchrotron Radiat. 2009;16:513–523.
[7] Bromiley GD, Redfern SAT, Le Godec Y, Hamel G, Klotz S. A portable high-pressure stress cell based on the V7 Paris–Edinburgh apparatus. High Pressure Res. 2009;29:306–316.
[8] Fang J, Bull CL, Hamidov H, et al. A rotator for single-crystal neutron diffraction at high pressure. Rev Sci Instrum. 2010;81:113901-6.
[9] Wang Y, Uchida T, Westferro F, Rivers ML, et al. High-pressure X-ray tomography microscope: synchrotron computed microtomography at high pressure and temperature. Rev Sci Instrum. 2005;76:073709-1-6.
[10] Lesher CE, Wang Y, Gaudio S, Clark A, Nishiyama N, Rivers M. Volumetric properties of magnesium silicate glasses and supercooled liquid at high pressure by X-ray microtomography. Phys Earth Planet Inter. 2009;174:292–301.
[11] Wang YB, Lesher C, Fiquet G, et al. *In situ* high-pressure and high-temperature X-ray microtomographic imaging during large deformation: a new technique for studying mechanical behavior of multiphase composites. Geosphere. 2011;7:40–53.
[12] Philippe J, Le Godec Y, Bergame F, Morand M. French Patent INPI, 2012, number.
[13] Dobson DP, Mecklenburgh J, Alfe D, Wood IG, Daymond MR. A new belt-type apparatus for neutron-based rheological measurements at gigapascal pressures. High Pressure Res. 2005;25:107–118.
[14] Yamazaki D, Karato S-i. High-pressure rotational deformation apparatus to 15 GPa. Rev Sci Instrum. 2001;72:4207–4211.
[15] Kono Y, Kenney-Benson C, Shibazaki Y, Park C, Wang Y, Shen G. X-ray imaging for studying behavior of liquids at high pressures and high temperatures using Paris–Edinburgh press. Rev Sci Instrum. 2015;86:072207-1-8.
[16] ESRF Experimental Report ES 92; 2014.
[17] ESRF Experimental Report MI 1086; 2013.
[18] SOLEIL Experimental Report n° 20140105; 2015.
[19] ESRF Experimental Report n° ES 33; 2014.
[20] Drakopoulos M, Connolley T, Reinhard C, et al. I12: the joint engineering, environment and processing (JEEP) beamline at diamond light source. J Synchrotron Radiat. 2015;22:828–838.
[21] Abràmoff MD, Magalhães PJ, Ram SJ. Image processing with imageJ. Biophoton Int. 2004;11:36–42.

[22] Yoshino T, Walter MJ, Katsura T. Connectivity of molten Fe alloy in peridotite based on in situ electrical conductivity measurements: implications for core formation in terrestrial planets. Earth Planet Sci Lett. 2004;222:625–643.
[23] Kim Y, Baek J, Hwang D. Ring artifact correction using detector line-ratios in computed tomography. Opt Express. 2014;22:13380–13392.
[24] Ketcham RA. Three-dimensional grain fabric measurements using high-resolution X-ray computed tomography. J Struct Geol. 2005;27:1217–1228.
[25] Kohlstedt DL, Holtzman BK. Shearing melt Out of the earth: An experimentalist's perspective on the influence of deformation on melt extraction. Annu Rev Earth Planet Sci. 2009;37:561–593.